Electronic Supplementary Information

Dominance of Unique P⋯π Phosphorus Bonding with π donors: Evidence Using Matrix Isolation Infrared Spectroscopy and Computational Methodology

Swaroop Chandra, B. Suryaprasad, N. Ramanathan* and K. Sundararajan

Homi Bhabha National Institute, Materials Chemistry & Metal Fuel Cycle Group,
Indira Gandhi Center for Atomic Research, Kalpakkam – 603102, Tamil Nadu, India

Corresponding author: nram@igcar.gov.in

Experimental results of PCl_3-C_2H_2 in N_2 matrix

In the experiments involving PCl_3 trapped within N_2 matrices, HCl consistently appeared as an impurity. The complete elimination of HCl was not successful, despite several efforts of purification. Consequently, heterodimers such as C_2H_2– HCl and C_2H_4–HCl were generated, along with heterotrimers such as HCl-PCl_3-C_2H_4. Computational traces of the potential energy surfaces (PESs) of C_2H_2-HCl, C_2H_4-HCl, HCl-PCl_3-C_2H_2 and HCl-PCl_3-C_2H_4 were performed at the MP2 level of theory with aug-cc-pVDZ as the basis set. Experimentally, the generation of HCl-PCl_3-C_2H_2 trimer was not observed, while HCl-PCl_3-C_2H_4 was observed. Serendipitously, the PES trace of trimer HCl-PCl_3-C_2H_4, revealed the lowest energy minimum to be stabilized by a concert of P…π and H-Cl…P, phosphorus bonding, with a cooperative contribution from C-H…Cl-P H-bonding, as revealed by the QTAIM plot in Figure S1.

Vibrational Assignments

Asymmetric C-H stretch region of C_2H_2

Figure S2 displays the asymmetric C-H stretch region of C_2H_2, trapped in N_2 matrix. Absorption feature at 3283.3 cm^{-1} corresponds to the v_3 asymmetric C-H stretch mode in C_2H_2.[1] Computations predicted a red shift of -10.4 cm^{-1} in the frequency associated with the asymmetric C-H stretch mode in C_2H_2–HCl heterodimer. In the IR spectrum, a feature at 3276.3 cm^{-1} (shift: -7.0 cm^{-1}) varied in intensity which was in sync with the concentration variation of the HCl impurity. Together with the acceptable agreement with the computed shift, this feature has been assigned to the HCl-C_2H_2 heterodimer in N_2 matrix. The harmonic frequency calculations performed on PAc I and II predicted a red-shift of -5.9 and -6.7 cm^{-1}, respectively in the frequencies associated with the asymmetric C-H stretching modes of C_2H_2 within the heterodimers. A similar closeness in the shifts was observed in the harmonic frequency calculations at the CCSD level too (Table S2). In the IR spectrum, there appeared a feature at 3272.7 cm^{-1}, amounting to a red-shift of -10.6 cm^{-1}. The variation of the intensity against the concentration variations introduced in terms of the PCl_3 precursor, allow the cautious assignment of this feature to PAc I and/or PAc II. The absorption features at 3270.6 and 3265.3 cm^{-1}, exhibit a mutual dependence on their respective intensity variations, as seen in Figure S2. The PES trace of the $(C_2H_2)_2$-PCl_3 heterotrimer predict a red-shift of -9.5 and -17.8 cm^{-1} in the frequency associated with the C-H stretch mode in the proton acceptor C_2H_2 and proton donor C_2H_2, respectively. This is in acceptable agreement with the observed shifts of -12.7 and -18.0 cm^{-1}, for the absorption features at 3270.6 and 3265.3 cm^{-1}. These have been assigned to the 2:1 heterotrimer of C_2H_2:PCl_3. It is important to note the absence of the features at 3279.2 and 3257.0 cm^{-1}, corresponding to the asymmetric C-H stretch in C_2H_2 homodimer.[1]

Asymmetric C-H stretch region of C_2H_4

The asymmetric C-H stretch region of C_2H_4 trapped in N_2 matrix (Figure S3 Left), shows an absorption feature at 2986.8 cm^{-1} which exhibits a clear dependence on the concentration of the PCl_3 precursor. With respect to the absorption feature corresponding to the ν_{11} asymmetric C-H stretch mode of C_2H_4 at 2989.7 cm^{-1},[2] the aforementioned feature is red-shifted by -2.9 cm^{-1}. This is in excellent agreement with the predicted shift of -2.5 cm^{-1} at MP2/aug-cc-pVDZ. Thus, the new absorption feature at 2986.8 cm^{-1} has been assigned to PEth I in N_2 matrix.

C-H bend region of C_2H_4

As a consequence of annealing, two absorption features appear at 958.7 and 951.2 cm^{-1} in the C-H bending region of C_2H_4 (Figure S3 Right) is blue shifted by 11.8 and 4.3 cm^{-1} from the monomer absorption at 946.9 cm^{-1}.[2] The intensity of both the features varies with the concentration variations of the PCl_3 precursor. The harmonic frequency calculations of PEth I, predicted a blue shift of 5.0 cm^{-1} with respect to the ν_7 mode of C_2H_4, which is in acceptable agreement with the observed shift of 4.3 cm^{-1}. The computed shift associated with the C-H bending mode in the lowest energy minimum of C_2H_4 in $HCl-C_2H_4-PCl_3$ heterodimer is blue shifted by 19.8 cm^{-1}. This is quite off from the observed shift of 11.8 cm^{-1}. However, the dependence of the intensity on the concentration of the PCl_3 precursor allows the cautious assignment of this feature to the $HCl-C_2H_4-PCl_3$ heterotrimer.

Asymmetric P-Cl Stretch region

The ν_3 mode of $PCl_3(Cl^{35}:Cl^{37}::3:0)$ monomer absorption was observed at 496.6 cm^{-1}.[3] Two new features were observed at 495.1 cm^{-1} and 490.1 cm^{-1}(Figure S4) pick up in intensity as a consequence of annealing, and show concentration dependence on C_2H_4. The harmonic frequency calculations of PEth I predict a feature at 484.3 cm^{-1}, red shifted by -7.5 cm^{-1}, with respect to the ν_3 mode at 491.8 cm^{-1}. The computed red shift of -7.5 cm^{-1} agrees well with the experimental shift of -6.5 cm^{-1}. The frequency calculations on the lowest energy minimum on the PES of $HCl-PCl_3-C_2H_4$ heterotrimer revealed a red-shift of -1.2 cm^{-1}, associated with the asymmetric P-Cl stretch. This is in excellent agreement with the experimental red shift of -1.5 cm^{-1}, associated with the feature observed at 495.1 cm^{-1}, which proves the generation of the heterotrimer.

Table S1 presents a comprehensive list of all the assignments. Table S2 presents a comparison of the computed shifts at CCSD, MP2, B3LYP and B2PLYP levels of theory all with aug-cc-pVDZ basis sets, from the harmonic frequency calculations performed on all the minima on the PESs of PAc and PEth.

Justification for improbability in generation of $1:2::C_2H_2:PCl_3$ heterotrimers within matrices

The high concentration of PCl_3 raises the possibility of formation of $1:2::C_2H_2:PCl_3$ trimers. A computational trace of the respective PES at MP2/aug-cc-pVDZ level, revealed three minima (Figure S6). With respect to the global minimum, the 1st local has an excess energy of 0.90 kcal mol^{-1} while the 2nd local has energy of 1.24 kcal mol^{-1}. The shift in the frequency

associated with the global minimum is predicted to be -13.2 cm^{-1}. Compared to this, the predicted shifts of -9.8 and -17.8 cm^{-1} for the 2:1::C$_2$H$_2$:PCl$_3$ heterotrimer are much more consistent with the observed shifts of -10.1 and -16.7 cm^{-1}. Also, the relative intensities of two features (in both N$_2$ and Ar matrices) vary synchronously such that the ratio of their intensities is always the same. If it were the 1:2::C$_2$H$_2$:PCl$_3$ heterotrimer the presence of a single characteristic C-H stretch feature would conform its formation, unlike the twin features observed in the experiments, which confirms the generation of 2:1::C$_2$H$_2$:PCl$_3$ heterotrimers. Probing the P-Cl stretch region for this discrimination is not an option owing to the low computed shifts predicted for the geometries of both the scenarios: 1:2 or 2:1 C$_2$H$_2$:PCl$_3$ heterotrimers, hindering their discernment due to the overcrowding of the P-Cl region by the isotopic signatures of PCl^{35}Cl$_2$^{37} and PCl$_2$^{35}Cl^{37}.
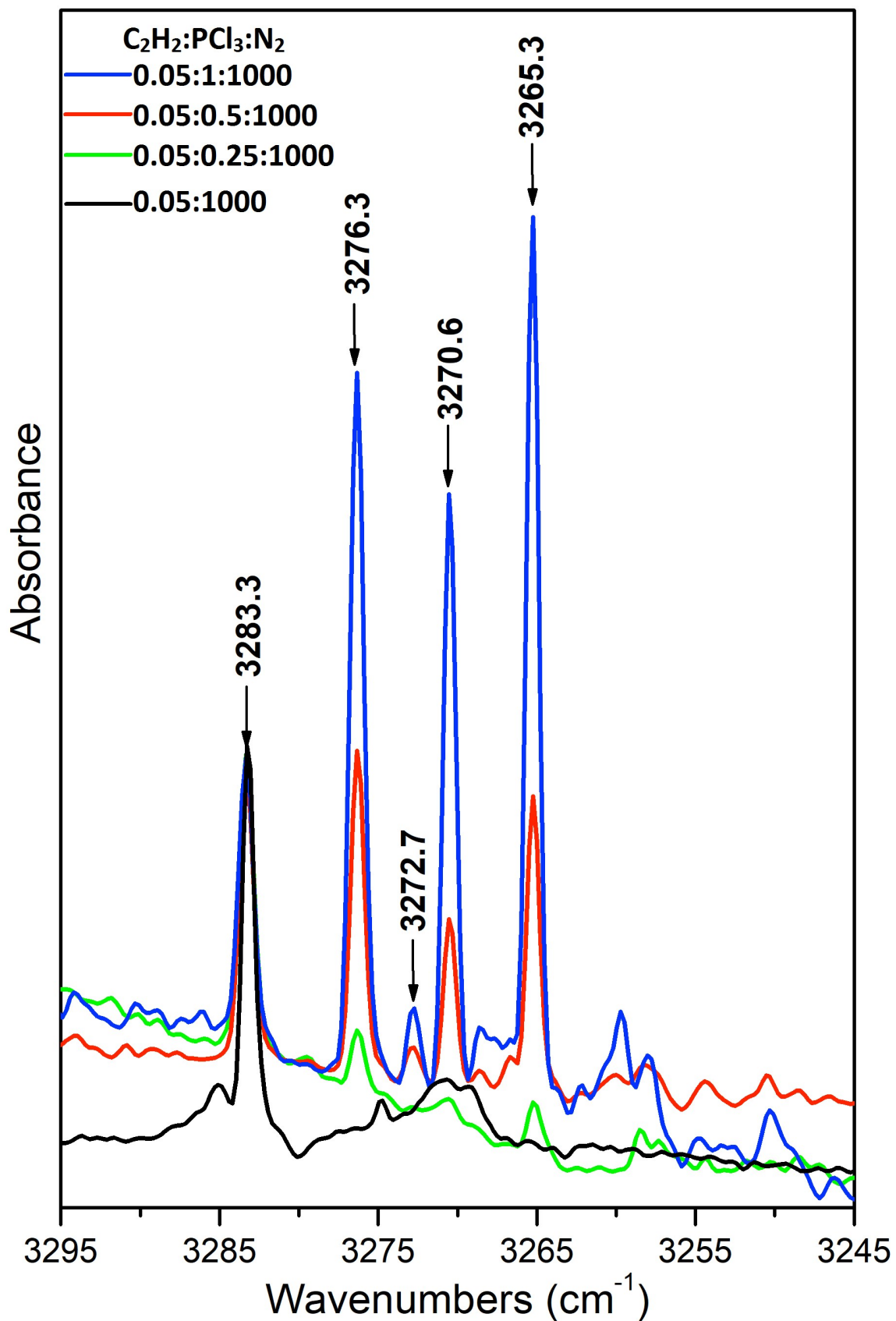
Figure S1. Infrared spectra of asymmetric C-H stretch region of C_2H_2 correspond to the co-deposition experiments of PCl_3 and C_2H_2 in N_2 matrix. All spectra were recorded at 12 K after annealing the matrix to 32 K.
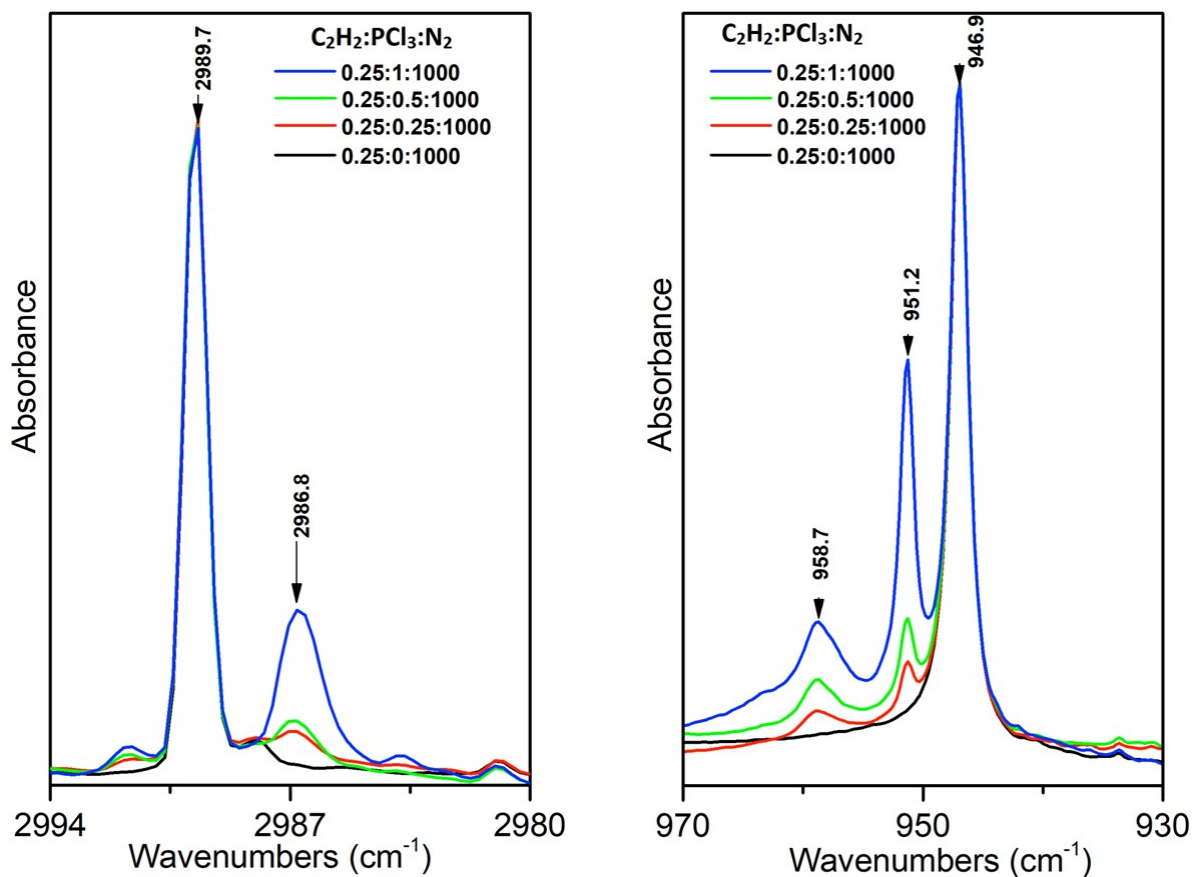
Figure S2. FT-IR spectra of C-H bending region. Grid A and Grid B correspond to the experiments of PCl_3 with C_2H_2 and C_2H_4 in N_2 matrix. All spectra were recorded at 12 K after annealing the matrix to 32 K.
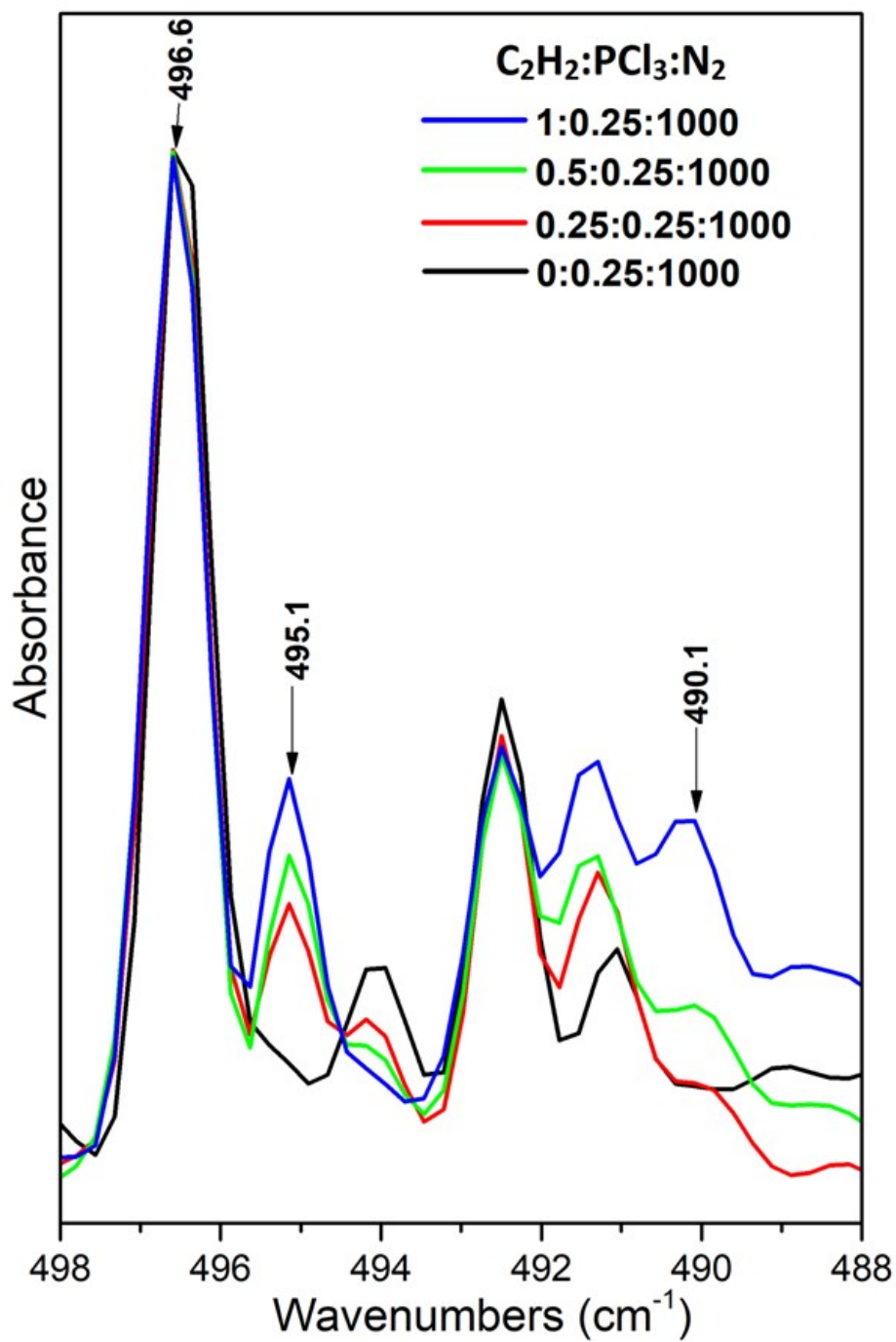
Figure S3. Infrared spectra of asymmetric P-Cl stretching region of PCl_3 with C_2H_2 in N_2 matrix. All spectra were recorded at 12 K after annealing the matrix to 32 K.
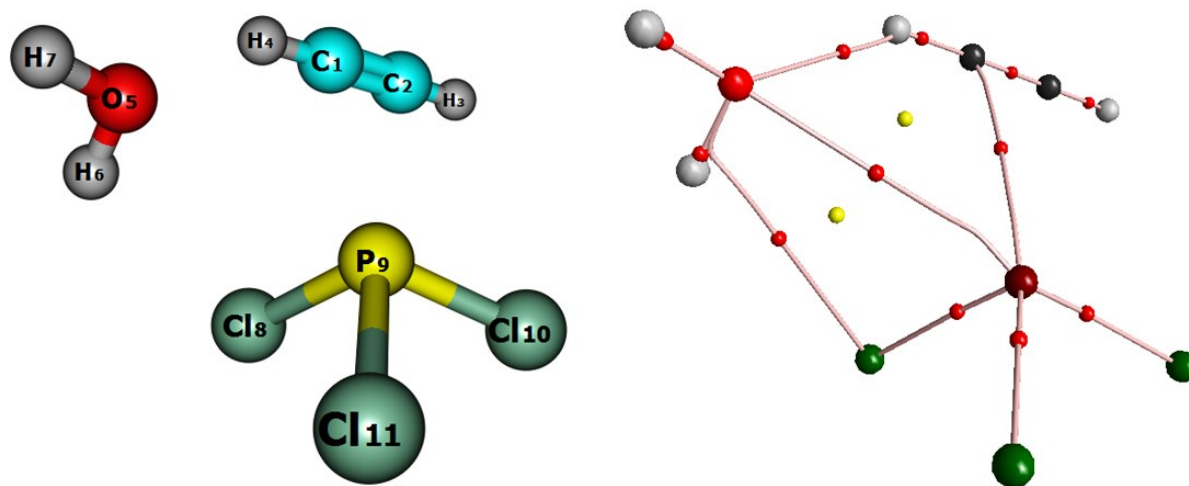
Figure S4. $PCl_3 - C_2H_4 - H_2O$ heterotrimer computed at MP2/aug-cc-pVDZ level of theory
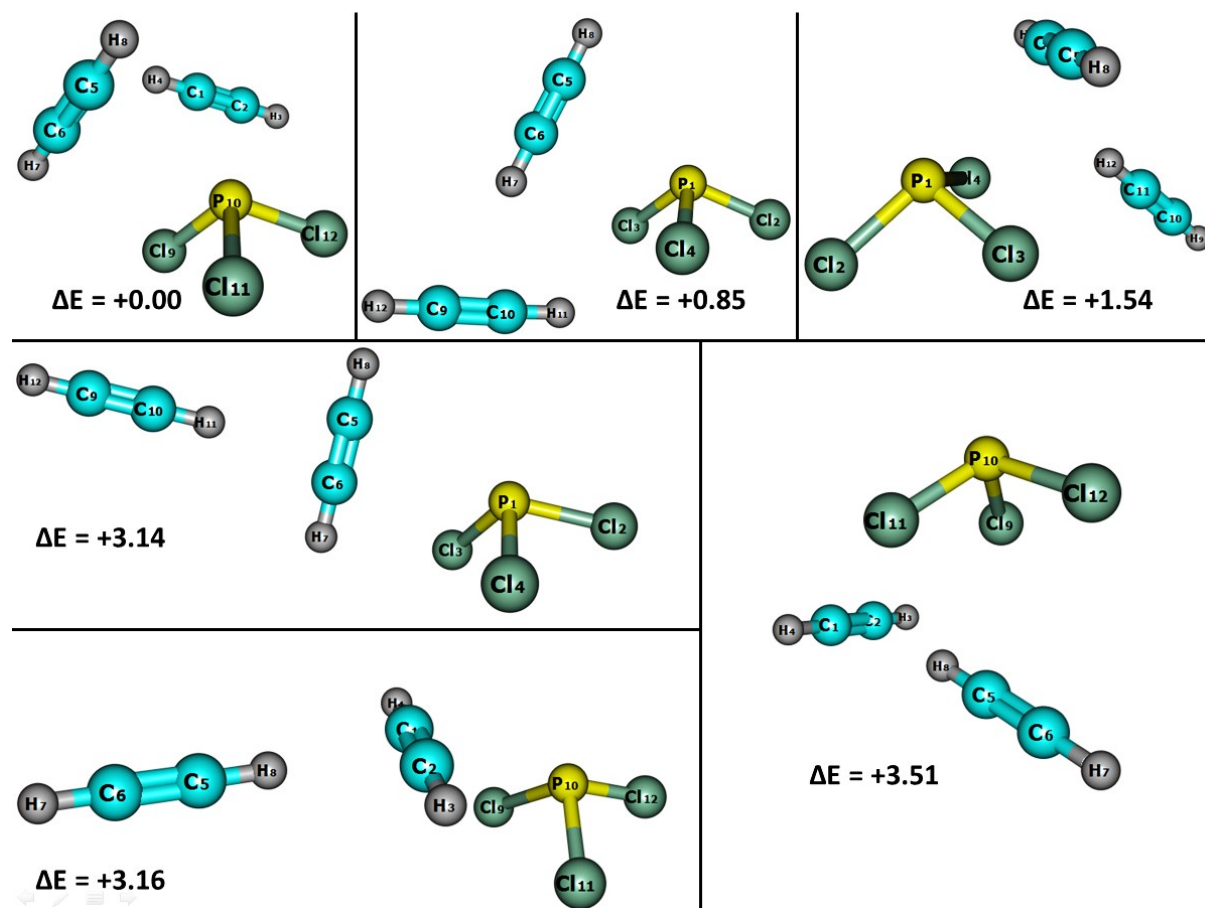
Figure S5. Optimized geometries of 2:1 $C_2H_2:PCl_3$ heterotrimers computed at MP2/aug-cc-pVDZ level of theory and their respective relative ZPE energies (kcal mol^{-1})

Figure S6. Optimized geometries of minima on the PES of 1:2::C_2H_2:PCl_3 heterotrimers

Figure S7. PCl$_3$-C$_2$H$_4$-HCl heterotrimer computed at MP2/aug-cc-pVDZ level of theory

Table S1. Computed and experimental vibrational wavenumbers (in N_2 matrix) and shifts of different vibrational modes of PAc I, PAc II and PEth I heterodimers computed at MP2 level of theory with aug-cc-pVDZ basis set.
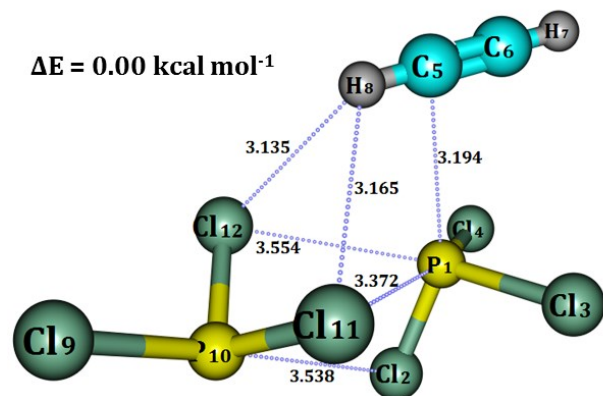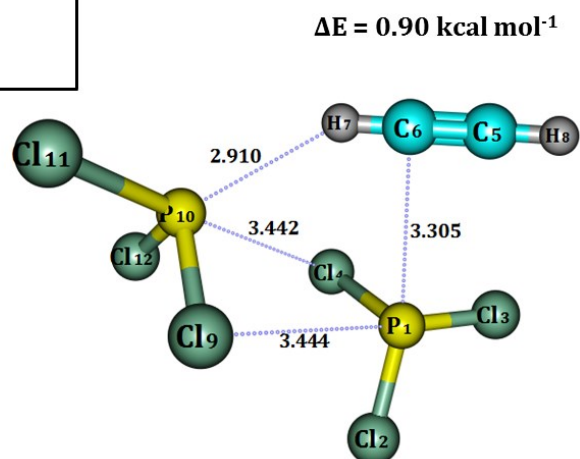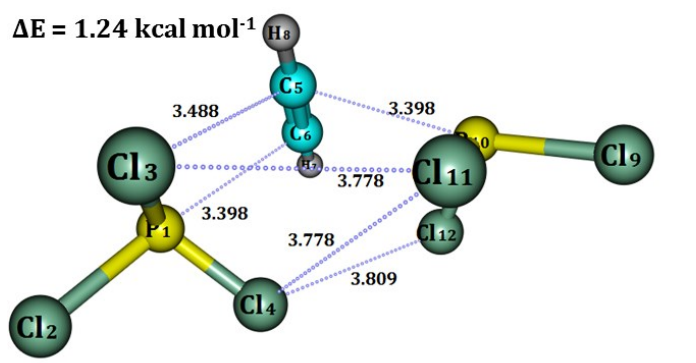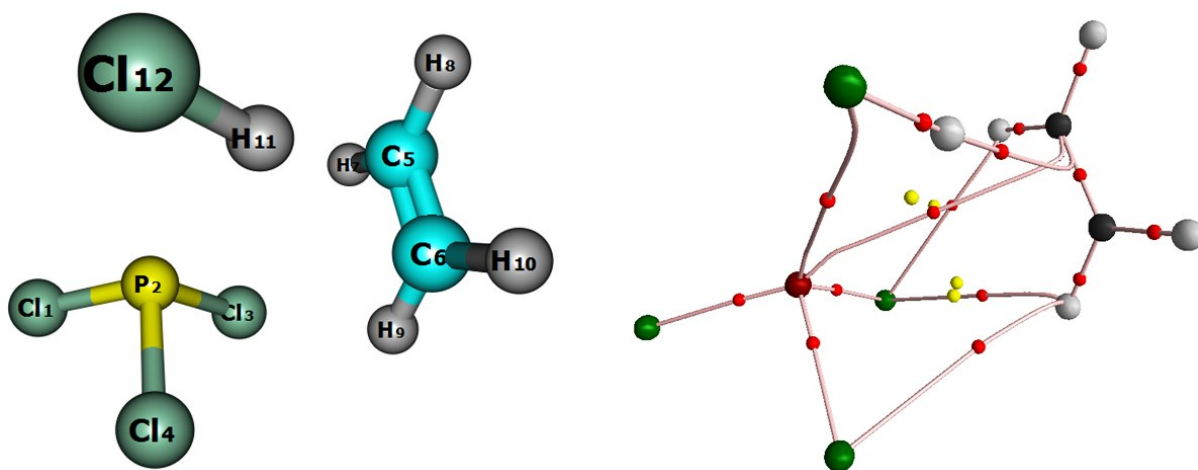
Computed Wavenumber(cm^{-1})		Experimental Wavenumber(cm^{-1})		Mode Assignment
ν	$\Delta\nu$	ν	$\Delta\nu$	
P-Cl Stretch Region				
491.8 (146.8)	---	496.6	---	ν_3 of PCl_3 monomer
486.5 (172.8)	-5.3	---	---	Asymm P-Cl stretch in PAc I
487.0 (125.5)	-4.8	---	---	Asymm P-Cl stretch in PAc II
490.6 (136.1)	-1.2	495.1	-1.5	P-Cl stretch HCl-PCl_3-C_2H_2[a]
484.3 (181.1)	-7.5	490.1	-6.5	Asymm P-Cl stretch in PEth I
C-H Stretch region in C_2H_2				
3431.7 (93.3)	---	3283.3	---	ν_3 of C_2H_2 monomer
3421.3 (111.9)	-10.4	3276.3	-7.0	C_2H_2-HCl
3425.8 (90.2)	-5.9	3272.7	-10.6	Asymm C-H stretch PAc I
3425.0 (93.9)	-6.7	3272.7	-10.6	Asymm C-H stretch PAc II
3422.2 (95.5)	-9.5	3270.6	-12.7	Proton acceptor $(C_2H_2)_2$ - PCl_3[a]
3413.9 (95.5)	-17.8	3265.3	-18.0	Proton donor $(C_2H_2)_2$ - PCl_3[a]
C-H Stretch region in C_2H_4				
3175.7 (11.4)	---	2989.7	---	ν_{11} C_2H_4
3173.2 (4.9)	-2.5	2986.8	-2.9	Asymm C-H stretch PEth I
C-H Bend region in C_2H_4				
979.2 (95.0)	---	946.9	---	ν_7 of C_2H_4 monomer
984.2 (119.8)	+5.0	951.2	+4.3	C-H bend in PEth I
999.0 (114.0)	+19.8	958.7	+11.8	C-H bend in C_2H_4-HCl

[a]Asymmetric stretch

Table S2. Computed Shifts of PCl_3 with C_2H_2 and C_2H_4 heterodimers at CCSD level of theory

CCSD/aug-cc-pVDZ	Computed Wavenumber (Shift) cm^{-1}	Intensity (km mol^{-1})
PCl_3		
Asymm.Stretch (v_3)	493.0	136.8
C_2H_2		
Asymm.Stretch (v_3)	3404.7	80.1
Bending[a] (v_5)	713.4	93.4
C_2H_4		
Bending[a] (v_7)	975.9	91.1
PAc - I		
Asym P-Cl Stretch	488.8(-4.2)	155.8
Asym C-H Stretch	3400.8(-3.9)	77.0
C-H Bend[a]	709.3(-4.1)	99.1
PAc - II		
Asym P-Cl Stretch	489.6(-3.4)	119.3
Asym C-H Stretch	3400.2(-4.5)	79.7
C-H Bend[a]	711.8(-1.6)	77.9
PAc - III		
Asym P-Cl Stretch	485.6(-7.5)	113.0
Asym C-H Stretch	3408.9(4.2)	125.1
C-H Bend[a]	743.6(30.2)	75.2
PEth - I		
Asym P-Cl Stretch	488.2(-4.8)	132.8
C-H Bend	982.7(+6.8)	114.2
PEth – II		
Asym P-Cl Stretch	490.3(-2.7)	122.1
C-H Bend	979.6(+3.7)	67.6
PEth – III		
Asym P-Cl Stretch	491.8(-1.2)	153.8
C-H Bend	975.7(-0.2)	79.8

[a]Out of plane bending

Table S3. Computed Shifts of PCl_3 with C_2H_2 and C_2H_4 heterodimers at MP2 level of theory

MP2/aug-cc-pVDZ	Computed Wavenumber (Shift) cm^{-1}	Intensity (km mol^{-1})
PCl$_3$		
Asymm.Stretch (ν_3)	491.8	146.8
C$_2$H$_2$		
Asymm.Stretch (ν_3)	3431.7	93.3
Bending^a (ν_5)	703.0	94.6
C$_2$H$_4$		
Bending^a (ν_7)	979.2	95.0
PAc - III		
Asym P-Cl Stretch	494.5(+2.4)	112.9
Asym C-H Stretch	3432.8(+1.1)	149.2
C-H Bend^a	730.6(+27.6)	77.7
PEth – II		
Asym P-Cl Stretch	488.8(-3.0)	130.8
C-H Bend	980.8(+1.6)	70.1
PEth – III		
Asym P-Cl Stretch	490.5(-1.3)	164.9
C-H Bend	977.6(-1.6)	82.6

^{a}Out of plane bending

Table S4: Computed Shifts of PCl_3 with C_2H_2 and C_2H_4 heterodimers at B3LYP-GD3 level of theory[a]

B3LYP-GD3/aug-cc-pVDZ	Computed Wavenumber (Shift) cm^{-1}	Intensity (km mol^{-1})
PCl$_3$		
Asymm.Stretch (v_3)	464.4	146.3
C$_2$H$_2$		
Asymm.Stretch (v_3)	3416.0	95.4
Bending[b] (v_5)	727.4	100.5
C$_2$H$_4$		
Bending[a] (v_7)	982.4	99.5
PAc - I		
Asym P-Cl Stretch	458.7(-5.7)	170.9
Asym C-H Stretch	3413.6(-2.4)	89.7
C-H Bend[b]	726.7(-0.7)	113.4
PAc - II		
Asym P-Cl Stretch	459.2(-5.2)	127.7
Asym C-H Stretch	3412.9(-3.1)	93.2
C-H Bend[b]	724.7(-2.7)	81.7
PAc - III		
Asym P-Cl Stretch	466.9(+2.5)	129.7
Asym C-H Stretch	3415.2(-0.8)	148.4
C-H Bend[b]	737.2(+9.8)	86.8
PEth - I		
Asym P-Cl Stretch	458.3(-6.6)	173.6
C-H Bend	994.7(+12.3)	95.5
PEth – II		
Asym P-Cl Stretch	461.8(-3.7)	130.4
C-H Bend	986.8(+4.4)	64.1
PEth – III		
Asym P-Cl Stretch	464.4(-1.1)	165.3
C-H Bend	982.2(-0.2)	85.8

[a]The geometry of PAc IV could not be optimized at the B3LYP-GD3 level of theory. Hence, the computed shifts of the respective heterodimer have been omitted altogether.
[b]Out of plane bending

Table S5: Computed Shifts of minima at B2PLYP level of theory

B2PLYP/aug-cc-pVDZ	Computed Wavenumber (Shift) cm^{-1}	Intensity (km mol^{-1})
PCl$_3$		
Asymm.Stretch (ν_3)	477.6	145.9
C$_2$H$_2$		
Asymm.Stretch (ν_3)	3431.6	97.2
Bending^a (ν_5)	722.2	102.3
C$_2$H$_4$		
Bending^a (ν_7)	985.2	98.1
PAc - I		
Asym P-Cl Stretch	470.9(-6.7)	171.0
Asym C-H Stretch	3428.5(-3.1)	89.6
C-H Bend^a	718.4(-3.8)	111.4
PAc - II		
Asym P-Cl Stretch	472.1(-5.5)	126.88
Asym C-H Stretch	3427.7(-3.9)	93.1
C-H Bend^a	722.1(-0.1)	80.5
PAc - III		
Asym P-Cl Stretch	479.0(+1.1)	129.4
Asym C-H Stretch	3431.6(0)	147.0
C-H Bend^a	734.1(+11.9)	83.3
PEth - I		
Asym P-Cl Stretch	471.3(-6.7)	168.5
C-H Bend	993.9(+8.7)	121.0
PEth – II		
Asym P-Cl Stretch	474.6(-3.4)	130.1
C-H Bend	989.0(+3.8)	69.8
PEth – III		
Asym P-Cl Stretch	477.1(-0.9)	164.8
C-H Bend	984.2(-1.0)	84.0

^{a}Out of plane bending

Table S6: Relevant intermolecular charge transfer among PCl_3 and C_2H_2 in PAc I dimer

PAc I				
Perturbation Energies			**Occupancies**	
Donor	**Acceptor**	**E_2^a**	**Donor**	**Acceptor**
σP1Cl4	π*(2)C5C6	0.05	1.99060(1.99092)	0.00284(0.00903)
n(2)Cl3	σ*C5C6	0.07	1.96659(1.96762)	0.00065(0.00000)
n(2)Cl3	πC5C6	0.05	1.96659(1.96762)	0.00938(0.00000)
n(2)Cl3	π*(2)C5C6	0.39	1.96659(1.96762)	0.00284(0.00903)
n(3)Cl3	σ*C5C6	0.06	1.95670(1.95567)	0.00065(0.00000)
n(3)Cl3	π*(2)C5C6	0.14	1.95670(1.95567)	0.00284(0.00903)
n(2)Cl4	σ*C5C6	0.07	1.96661(1.96765)	0.00065(0.00000)
n(2)Cl4	πC5C6	0.06	1.96661(1.96765)	0.00938(0.00000)
n(2)Cl4	π*(2)C5C6	0.41	1.96661(1.96765)	0.00284(0.00903)
n(3)Cl4	σ*C5C6	0.07	1.95677(1.95571)	0.00065(0.00000)
n(3)Cl4	π*(2)C5C6	0.15	1.95677(1.95571)	0.00284(0.00903)
π(2)C5C6	σ*P1Cl2	2.54	1.99005(1.99230)	0.07112(0.06818)
π(2)C5C6	σ*P1Cl3	0.05	1.99005(1.99230)	0.06894(0.06816)
π(2)C5C6	σ*P1Cl4	0.05	1.99005(1.99230)	0.06902(0.06818)

^{a}in kcal mol^{-1}

Table S7: Relevant intermolecular charge transfer among PCl_3 and C_2H_2 in PAc II dimer

PAc II				
Perturbation Energies			**Occupancies**	
Donor	**Acceptor**	**E_2^a**	**Donor**	**Acceptor**
σP1Cl3	π*(2)C5C6	0.07	1.99037(1.99092)	0.00284(0.00903)
σP1Cl4	π*(2)C5C6	0.07	1.99037(1.99092)	0.00284(0.00903)
nP1	π*(2)C5C6	0.07	1.99551(1.99762)	0.00284(0.00903)
n(2)Cl3	σ*C5C6	0.07	1.96744(1.96762)	0.00075(0.00000)
n(2)Cl3	π*(2)C5C6	0.15	1.96744(1.96762)	0.00284(0.00903)
n(3)Cl3	σ*C5C6	0.08	1.95631(1.95567)	0.00075(0.00000)
n(3)Cl3	π*(2)C5C6	0.26	1.95631(1.95567)	0.00284(0.00903)
n(2)Cl4	σ*C5C6	0.07	1.96744(1.96765)	0.00075(0.00000)
n(2)Cl4	π*(2)C5C6	0.15	1.96744(1.96765)	0.00284(0.00903)
n(3)Cl4	σ*C5C6	0.08	1.95631(1.95571)	0.00075(0.00000)
n(3)Cl4	π*(2)C5C6	0.26	1.95631(1.95571)	0.00284(0.00903)
π(2)C5C6	σ*P1Cl2	2.63	1.98991(1.99230)	0.07192(0.06818)
π(2)C5C6	σ*P1Cl3	0.05	1.98991(1.99230)	0.06882(0.06816)
π(2)C5C6	σ*P1Cl4	0.05	1.98991(1.99230)	0.06882(0.06818)

^{a}in kcal mol^{-1}

Table S8: Relevant intermolecular charge transfer among PCl_3 and C_2H_4 in PEth I dimer

PEth I				
Perturbation Energies			**Occupancies**	
Donor	**Acceptor**	**E_2^a**	**Donor**	**Acceptor**
σP2Cl4	π*C5C6	0.11	1.98995(1.99085)	0.00474(0.00246)
P2	π*C5C6	0.41	1.99434(1.99753)	0.00474(0.00246)
n2Cl3	σ*C5H7	0.14	1.96778(1.96728)	0.00856(0.00820)
n2Cl3	σ*C5H8	0.08	1.96778(1.96728)	0.00838(0.00820)
n3Cl3	σ*C6H9	0.12	1.95718(1.95535)	0.0083(0.00820)
n3Cl3	σ*C6H10	0.05	1.95718(1.95535)	0.0082(0.00820)
n2Cl4	π*C5C6	0.56	1.96624(1.96732)	0.00474(0.00246)
n3Cl4	π*C5C6	0.63	1.9562(1.95538)	0.00474(0.00246)
πC5C6	σ*Cl1P2	3.88	1.98351(1.99234)	0.07515(0.06900)
πC5C6	σ*P2Cl3	0.1	1.98351(1.99234)	0.06949(0.06894)
πC5C6	σ*P2Cl4	0.05	1.98351(1.99234)	0.06856(0.06894)

^{a}in kcal mol^{-1}

Table S9: Relevant intermolecular charge transfer among PCl_3 and C_6H_6 in PB I dimer

C6H6 - PCl3				
Perturbation Energies			**Occupancies**	
Donor	**Acceptor**	**E_2^a**	**Donor**	**Acceptor**
πC1C3	σ*P13Cl14	0.42	1.65434(1.66399)	0.07805(0.06893)
πC1C3	σ*P13Cl15	3.6	1.65434(1.66399)	0.08025(0.06893)
πC5C7	σ*P13Cl14	1.38	1.65549(1.66399)	0.07805(0.06893)
πC5C7	σ*P13Cl15	0.56	1.65549(1.66399)	0.08025(0.06893)
πC5C7	σ*P13Cl16	0.2	1.65549(1.66399)	0.07805(0.06893)
πC9C11	σ*P13Cl14	0.09	1.65550(1.66399)	0.07805(0.06893)
πC9C11	σ*P13Cl16	1.28	1.65550(1.66399)	0.07805(0.06893)
π*C1C3	σ*P13Cl15	2.53	0.33479(0.33235)	0.08025(0.06893)
π*C5C7	σ*P13Cl15	3.23	0.32869(0.33235)	0.08025(0.06893)
π*C9C11	σ*P13Cl15	0.31	0.32823(0.33235)	0.08025(0.06893)
σP13Cl16	π*C5C7	0.05	1.99043(1.99085)	0.32869(0.33235)
n2Cl14	π*C1C3	0.19		0.33479(0.33235)
n2Cl16	π*C5C7	0.29		0.32869(0.33235)
n3Cl16	π*C1C3	0.06		0.33479(0.33235)

^{a}in kcal mol^{-1}

Table S10: Results from the Fragment Analysis of selected minima on the PESs of the heterodimers using ADF-2016 package. All values are expressed in kcal mol^{-1}

Heterodimer	Attractive			Repulsive	
	Electrostatic	Orbital	Dispersion	Steric	Pauli Repulsion
PAc I	-4.34	-2.14	-2.87	2.8	7.14
PAc II	-7.2	-2.02	-2.82	1.75	8.96
PAc III	-0.29	-1.43	-2.57	2.76	3.06
PEth I	-5.7	-3.15	-3.68	4.4	10.09
PEth II	-1.69	-0.92	-3.69	2.72	4.41
PEth III	-0.44	-0.35	-1.25	0.81	1.25
PB I	-10.46	-6.2	-5.89	9.26	19.72
PB II	-5.04	-1.75	-7.01	5.72	10.76
PB IV	-2.21	-1.35	-4.7	3.92	6.13

References:

1   K. Sundararajan and K. S. Viswanathan, *J. Mol. Struct.*, 2006, **798**, 109–116.
2   H. Frei, *J. Chem. Phys.*, 1983, **79**, 748–758.
3   P. R. Joshi, N. Ramanathan, K. Sundararajan and K. Sankaran, *J. Phys. Chem. A*, 2015, **119**, 3440–3451.